Experimental Thermal and Fluid Science 58 (2014) 180–187

Contents lists available at ScienceDirect

Experimental Thermal and Fluid Science

journal homepage: www.elsevier.com/locate/etfs

Experimental study on cooling performance of a steam-cooled turbine blade with five internal cooling smooth channels

Liang Xu [a], Wei Wang [b], Tieyu Gao [c,*], Xiaojun Shi [a], Jianmin Gao [a], Wanyin Liang [a]

[a] State Key Laboratory for Manufacturing Systems Engineering, Xi'an Jiaotong University, No. 28, Xianning West Road, Xi'an, Shaanxi, PR China
[b] Taiyuan University of Technology, No. 79 West Yingze Street, Taiyuan, Shanxi, PR China
[c] Department of Thermal Power Engineering, Xi'an Jiaotong University, No. 28, Xianning West Road, Xi'an, Shaanxi 710049, PR China

ARTICLE INFO

Article history:
Received 25 October 2013
Received in revised form 4 July 2014
Accepted 4 July 2014
Available online 11 July 2014

Keywords:
Gas turbine
Steam cooling
Cooling efficiency
Internal cooling

ABSTRACT

Advanced cooling technology is a key measure of thermal protection for turbine blades, and raising inlet gas temperature of gas turbines. Using steam as a coolant in the internal cooling channels of turbine blade can significantly reduce the consumption of air drawn from the compressors and the closed circuits convective steam cooling can help to avoid the mixing loss between the mainstream and the cooling air so as to raise the overall efficiency of gas turbine. In this study, cooling performance comparison between the steam and air is conducted on a test blade with five smooth radial convective cooling channels. The temperature and static pressure on the surface of the mid-span of the test blade are measured and the cooling performance of the blade under different cooling conditions is evaluated. Results show that the middle region of the test blade has the highest cooling effectiveness, and then the leading edge follows. The cooling effectiveness at the trailing edge is the lowest. At the same mass flow rate, the averaged cooling effectiveness of steam cooling is higher than air by about 0.12. To obtain a similar cooling performance, the consumption of cooling steam is only 40.82% of the cooling air. In conclusion, steam cooling can achieve a better cooling performance than air, and improvements of cooling structure for the trailing edge is required for steam-cooling application in the given configuration.

1. Introduction

Although thermal efficiency and power of gas turbines increase with the increase of the inlet temperature, it is still a formidable challenge for researchers and designers of gas turbines to figure out how to keep turbine blades operating reliably and stably even under poor conditions like high-temperature and heavy-load. Advanced cooling technology, as a major means of thermal protection for turbine blades, is a key measure to the enhance inlet gas temperature of gas turbine. Nowadays, air has been the most commonly used coolant in turbine blade cooling. So far, the air cooling structure has been diversely combined with various approaches such as enhanced convective cooling with internal ribbed channels, jet impingement cooling, column group convective cooling, laminate plates cooling, transpiration cooling and all film-mulching cooling [1–9]. There are abundant research papers studying the air cooling for the turbine blade. The most systematic and complete study is made by Hylton et al. [10]. They made analytical and experimental evaluation of the heat transfer distribution of the heat transfer distribution over the surfaces of turbine vanes. Nevertheless, the air cooling has some drawbacks. For example, it not only consumes the high-pressure air drawn from the gas compressor but also impairs the turbine efficiency due to the mixing of cooling air with high-temperature mainstream in the cascade passages. There are two ways to solve the above problem: developing new structures or replacing air with another medium as coolant. Sophisticated and complex air cooling structure may lead to insurmountable manufacturing difficulties and high manufacturing costs. Thus new coolants have to be found and developed to make a technical breakthrough while a lot of efforts are being made to research and develop new cooling structures. Other alternative coolant like water, steam, steam spray, oil has been used widely for various equipments in the industry field.

As another alternative coolant, steam has already been used as coolant for the gas turbine blade cooling. For example, the H-serious gas turbines of GE [11], W501G steam-gas-fired combined-type of Siemens [12], Mitsubishi M701G2 gas turbine [13], and combined cycle power system of new generation "H System TM" of Toshiba [14]. Their high-temperature blades have one thing in common. Namely, they all employ steam cooling. The currently satisfactory operation experience of the last decade indicates that

* Corresponding author. Tel./fax: +86 29 82664103.
E-mail address: sunmoon@mail.xjtu.edu.cn (T. Gao).

http://dx.doi.org/10.1016/j.expthermflusci.2014.07.004
0894-1777/

steam cooling can remarkably improve the performance of gas turbines [15,16]. What makes steam cooling different from the traditional air cooling lies in the fact that the blade internal channels of steam cooling in closed circuits are used to prevent steam coolant from injecting into the cascade passages. Cooling steam is extracted from the exhaust of the steam turbine to reduce the temperature of the components related and to absorb heat through the cooling channels made on first blades and the outer cover of the gas turbine. After that, the cooling steam is discharged and inducted to mix up with the reheated steam flow from the heat recovery boiler to operate by expanding itself in the low pressure cylinder of the steam turbine. It has been proved that steam cooling used in the turbine internal cooling blade can significantly reduce the consumption of high-pressure air coolant and that the closed circuits of the steam coolant can reduce the cooling air that flows into the cascade passages, consequently reducing the loss caused by the mixing of high-temperature mainstream with the cooling air. Compared with air, steam has a higher specific heat and a better heat transfer performance, hence indicating a better cooling effect than air when they have a similar cooling structure. Steam cooling on turbine blades has such advantages as fast cooling speed, high cooling efficiency, simple structure, and is thus expected to play an important role in the research on state-of-the-art gas turbines.

Despite a lot of literature [17–20] that reports advantages of steam cooling in combined cycle units, there were few literatures that discuss the characteristics of heat transfer and flow of steam in the turbine steam-cooled blades. Nomato et al. [21] reported a simple internal steam cooling structure, in which about 30 radial cylindrical holes for steam cooling were located around the test blade. They suggest that high-pressure steam can replace air as a coolant because its cooling effect is efficient enough. Henderson [22] made an experimental research on analysis of using steam for cooling turbine blades. Pudupatty [23] made a comparison of the cooling effectiveness of superheated steam and hot air in internal turbine blade cooling. Bohn et al. [24,25] also designed an internal steam cooling structure, in which 21 radial cylindrical holes of various sizes for steam cooling were located in the blade inner cavity. Their experiments and numerical simulations of this steam cooling blade show that steam has a better cooling performance than air and the optimal effect was achieved when steam was in the medium pressure range. Nowak et al. [26] discussed the problem of blade cooling system optimization connected with conjugate heat transfer (CHT) analysis for reliable thermal field prediction within a steam cooled component. However, all of the above studies of steam cooling were focused on the cooling configuration of simple circular holes rather than the practical use of similar rectangular channels.

In the present study, we design a cooling structure for a real gas turbine blade, with five smooth internal cooling channels. These channels are rectangular and shaped like those conventionally used in most air cooling turbines blade rather than simple circular holes. A comparison of cooling effectiveness between steam cooling and air cooling is conducted. In addition, the effect of coolant temperature and mass flow rate on the cooling effectiveness is analyzed. At last, the limitations of this designed cooling structure, as well as steam cooling is discussed.

2. Experimental setup and method

Fig. 1 illustrates the experimental apparatus used to assess the internal convective cooling characteristics of the turbine blade. The experimental apparatus consists of a mainstream supply system, a cooling air supply system, a test section, a data acquisition system, a remote control system and an exhaust system. Four screw compressors are connected in parallel to supply the mainstream air with a maximum pressure of 0.8 MPa and a maximum mass flow rate of 3 kg/s. To simulate the high-temperature gas, the mainstream compressed air is blown into the air heater through a gas tank. In the air heater, the mainstream air can be arbitrarily heated and regulated linearly from the normal atmospheric temperature to 500 °C, with a regulation accuracy of ±2 °C. The cooling air is provided by a screw compressor with a maximum pressure of 0.8 MPa and a maximum mass flow rate of 0.2 kg/s. The cooling steam is provided by a steam generator with a maximum pressure of 1.0 MPa, a maximum steam superheated degree of 70 °C and a maximum mass flow rate of 0.16 kg/s. All the devices can be controlled by the remote control system. The data acquisition system can synchronously collect signals from the 70 pressure measuring points and the 230 thermocouples. The exhaust system can lower the exhaust temperature down to less than 150 °C and the noise down to less than 60 dB.

The cascade test section has three straight blades embedded in, shown in Fig. 2(a). The center blade is the test blade which has cooling structure and the other two are foil blades. These three blades have the same profile curve obtained by zooming out by half time the profile curve of the middle section in the first stage vane of a real heavy duty gas turbine. Detailed information about the test platform can be found in literature [27,28].

The test blade has five smooth rectangular internal cooling channels. These channels are named as duct 1, 2, 3, 4 and 5, respectively from the leading edge to the trailing edge of the blade. The geometry lines of the test blade cross-sections are shown in Fig. 2(b) and the detailed geometry of the test blade is described in Table 1 (see Table 2).

Fig. 3 illustrates the schematic of the test section and locations of the temperature and pressure measuring points. In the test section, the inlet width is 289 mm, the outlet width is 84.5 mm, and the airflow turning angle is 107°. A three-hole pressure probe is located at 240 mm upstream of the blade leading edge to measure

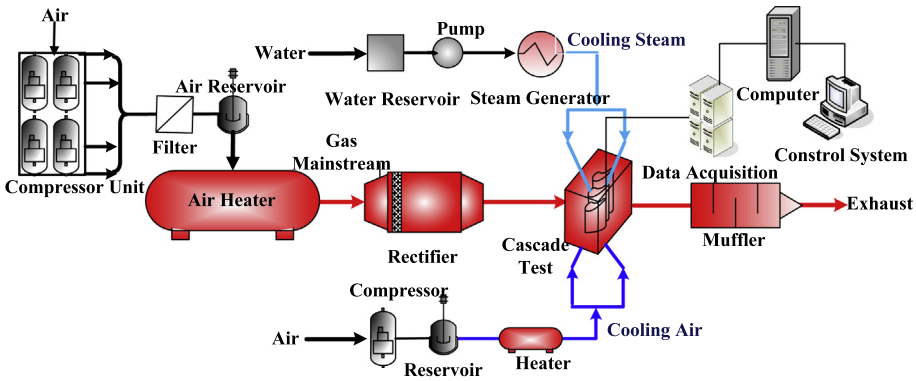

Fig. 1. Experimental apparatus for assessing the internal cooling characteristics of the turbine blade.

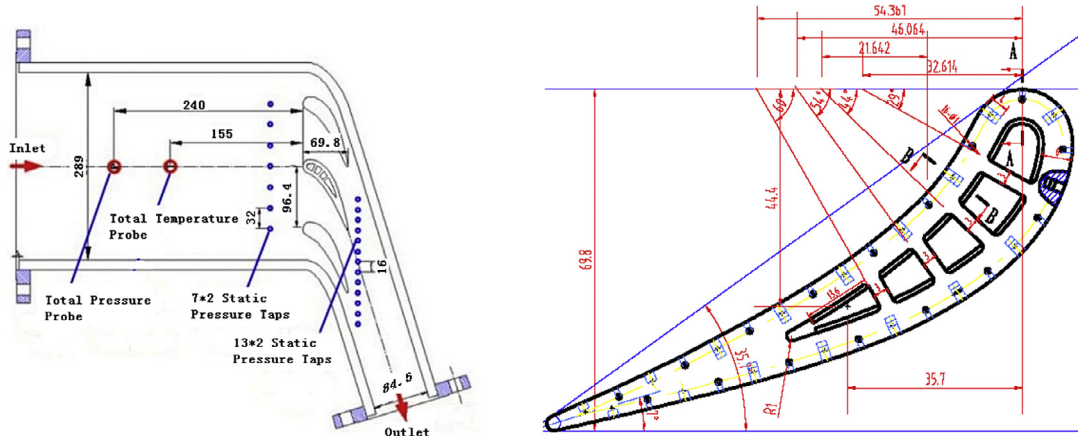

(a) Test section (b) Test blade

Fig. 2. Schematic of the test section and the test blade.

the total pressure of the inlet flow in the test section. A temperature probe is located at 155 mm upstream of the blade leading edge to measure the total temperature of the inlet flow in the test section. There are seven static pressure test taps located at the upper and lower end walls, respectively, about 25 mm upstream of the blade leading edge to measure the inlet static pressure of the cascade passage. Besides, 13 static pressure test taps are located at the upper and lower end walls and about 14 mm downstream of the trailing edge to measure the outlet static pressure of the cascade passage. Fig. 4 displays the 17 temperature measuring points and the 17 static pressure measuring points on the blade surface, which are located along the profile curve at the mid-span of the test blade and distance evenly with an interval of 7.5 mm between every two adjacent measuring points. The 17 pressure measuring points consist of one total pressure gauge and 16 differential pressure gauges. These pressure taps have a diameter of 1 mm and the thermocouples also have a diameter of 1 mm.

Table 1
Geometry of the test blade.

Parameters	Value
Hight (mm)	83
Pitch (mm)	96.4
Chord length (mm)	69.8
Outlet angle (°)	17
Thickness (mm)	6

Table 2
Geometry of the internal cooling ducts.

	Hydraulic diameter Dh (m)	Area ($10^{-5}m^3$)
Duct 1	0.0109	10.531
Duct 2	0.0099	9.125
Duct 3	0.0093	7.981
Duct 4	0.0087	6.891
Duct 5	0.0069	8.083

Those high-temperature pressure transducers have a nominal accuracy of ±0.075% of their full-scale range. Since the metal temperature on the surrounding areas of the cooled vane is high, the heat flux from these areas is not negligible, and heat conduction error must be estimated to obtain the accurate cooling effectiveness. The maximum uncertainty of wall temperature and gas temperature can be considered to be ±1.1 °C. The uncertainty regarding the measuring technique was estimated with a single sample uncertainty analysis based on the method proposed by Kline and McClintock [29]. So the conservative surface heat transfer coefficient uncertainty is less than 5%, which is considered acceptable for the current application.

The mainstream gas in the test section stays at a temperature of 420 °C. To minimize the heat loss the test section and all the pipes are wrapped with thick alumina-silicate layers and iron sheet.

3. Experimental operating conditions

When the heated mainstream airflow flows into the cascade test section through the rectifier, it has a turbulence rate of 5% and a temperature of 420 °C. The total mass flow rate of three

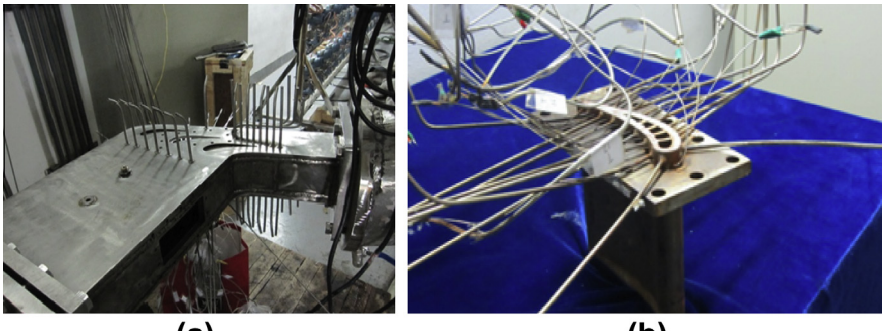

Fig. 3. Locations of the temperature and pressure measuring points on the blade section.

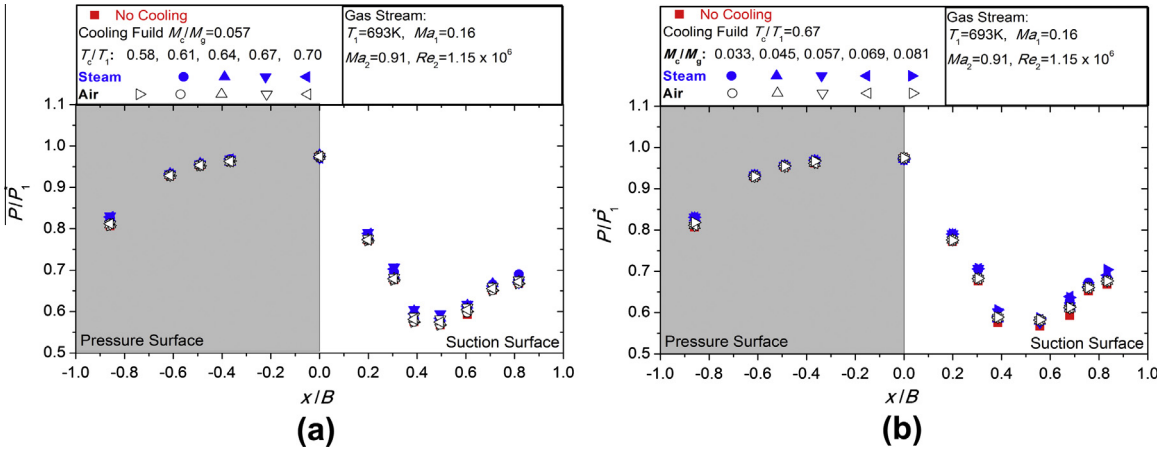

Fig. 4. Distribution of the surface static pressure on the middle section of the blade.

cascade passages in the test section is 2 kg/s. The mainstream airflow operating conditions in the test section are set as shown in Table 3.

Subscript 1 in Table 3 represents the inlet airflow parameters of the cascade passage and subscript 2 represents the outlet airflow parameters. The ε is the ratio of the cascade outlet static pressure to the cascade inlet total pressure. The plenum of the coolant at the upper end of the blade remains at around 200 kPa. Five various temperature and flow rate ratio are set for the coolant as is shown in Table 4.

Table 4
Operating condition of the coolant.

Cooling fluid	1	2	3	4	5
T_c/T_1	0.58	0.61	0.63	0.67	0.70
M_c/M_g	0.033	0.045	0.057	0.069	0.081

4. Results and discussion

4.1. Distribution of surface static pressure

Fig. 4 illustrates the distribution of the surface static pressure on the middle section of the blade. The abscissa is the relative axial chord length, which is equal to the ratio of the axial distance to the axial chord of the blade. The ordinate is the surface static pressure co-efficiency P/P_1 (the ratio of the surface static pressure to the total pressure at the inlet of the test section). The distribution of blade surface pressure shows a stagnation region at the leading edge of the test blade, where the velocity of the mainstream air is about zero and the static pressure coefficient is nearly 1. Downstream the stagnation region, the pressure begins to decrease. In the meanwhile, the high temperature airflow begins to expand and its velocity begins to increase. On the concave side of the blade (i.e. the pressure surface), the airflow expands and accelerates because of the adverse pressure gradient from the blade leading edge to the trailing edge. On the convex side of the blade (i.e. the suction surface), firstly the airflow expands and accelerates more rapidly. When the relative axial chord length (X/B) is 0.5, the static pressure coefficient reaches its minimum and the velocity of the airflow reaches its maximum. Then, from $X/B = 0.5$ to the trailing edge, the pressure increases whereas the velocity of the airflow decreases. Fig. 4(a) shows the static pressure distribution on the blade surface at five different coolant temperatures, and the mass flow rate of the coolant flow remains constant. Fig. 4(b) illustrates the static pressure distribution on the blade surface at five different coolant mass flow rates, and the coolant temperature remains constant. A comparison between the two figures shows that the internal cooling structure of the blade has no effect on the pressure distribution on the blade surface. And we can infer that the internal cooling structure of the blade does not have much impact on the external mainstream, consequently.

4.2. Thermal load of the blade

Fig. 5 shows the measured surface temperature distribution at the mid-span of the test blade. The abscissa is the relative axial chord length and the ordinate is T_w/T_1 (the ratio of blade surface temperature to the cascade inlet temperature). It can be seen from Fig. 5 that when the internal convective cooling is used, the temperature distribution on the pressure and the suction surfaces at the same axial distance are similar to each other. Nevertheless, there is indeed one difference between them. Namely, the temperature of the suction surface is lower than that of the pressure surface. When the relative axial chord length is 0.45, temperatures of both the pressure and suction surfaces are at their lowest. Under the joint action of a decrease in temperature at the leading edge and a slight decrease in temperature at the trailing edge, the temperature distribution curves look like an oblique "W" and are symmetric along the leading edge of the test blade.

Fig. 5(a) and (b) shows the wall temperature distribution at different coolant temperatures when the coolant mass flow rates is $M_c/M_g = 0.045$ and $M_c/M_g = 0.081$, respectively. The M_c means the mass flow rates of the coolant, and the M_g means the mass flow rates of the main gas in a single cascade passage. It indicates that the blade wall temperature drops significantly as the mass flow rate of the coolants increases as is expected. Compared with the condition where air coolant is used, the blade surface temperature

Table 3
Mainstream airflow condition parameters in the cascade test section.

Gas stream	T_1 (°C)	P_1 (kPa)	3 * M_g (kg s^{-1})	Ma_1	Ma_2	$Re2 \times 10^{-6}$	ε
Case	420	185.8	2.0	0.16	0.91	1.15	0.65

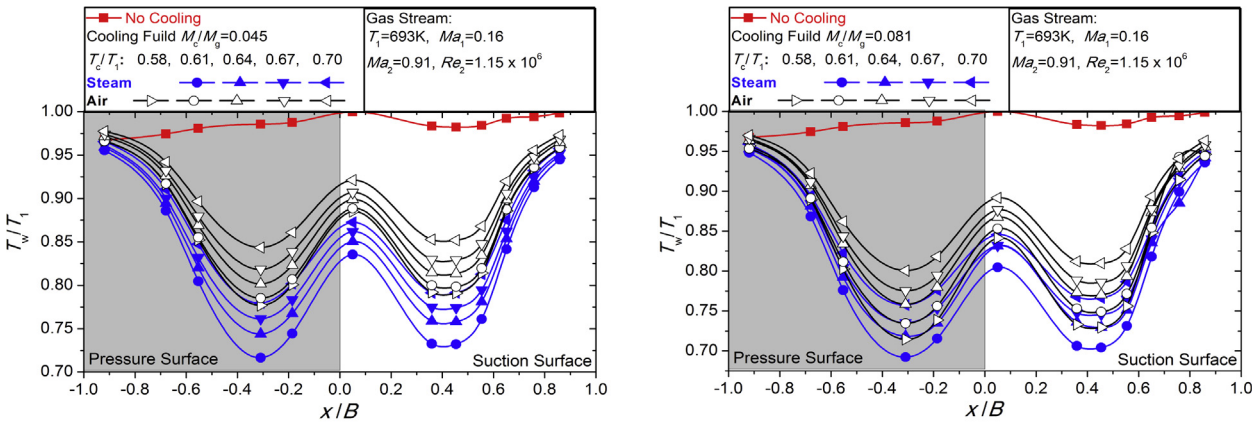

(a) Temperature distribution with different coolant temperatures at M_c/M_g=0.045

(b) Temperature distribution with different coolant temperatures at M_c/M_g=0.081

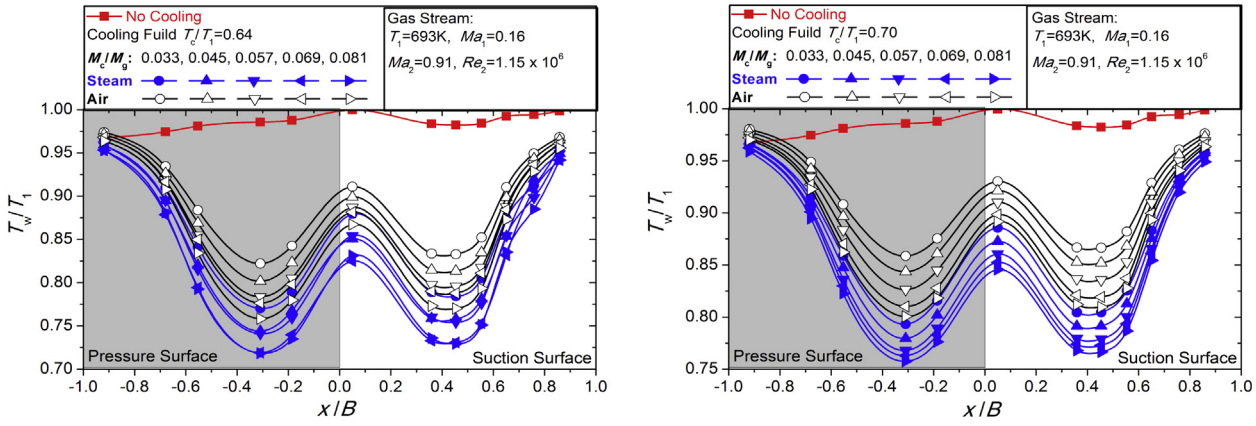

(c) Temperature distribution with different coolant mass Flow rates at T_c/T_g=0.64

(d) Temperature distribution with different coolant mass Flow rates at T_c/T_g=0.70

Fig. 5. Wall temperature distributions on the blade middle section.

decreases more significantly when steam coolant is used in a state similar to that of air coolant. When the mass flow rate of the coolant is small (M_c/M_g = 0.045), the cooling performance of air coolant cannot reach that of steam coolant unless the air coolant temperature is remarkably low. Fig. 5(c) and (d) shows the wall temperature distribution at different mass flow rates of the coolants when the coolant temperature is T_c/T_g = 0.64 and T_c/T_g = 0.70. As we expected, blade wall temperature decreases slowly as the coolant temperature increases. When the coolant temperature is high (where the coolant-mainstream temperature ratio is 0.7), the cooling performance of air cannot reach that of cooling steam unless the mass flow rate of air is remarkably high. From this we may infer that higher mass flow rate and lower temperature of the coolants can effectively reduce the wall temperature for the internal cooling method, and the cooling steam can lower the blade surface temperature more significantly than air.

To comprehensively evaluate the thermal load on the blade surface, two different kinds of parameters, viz. the average wall temperature (T_{aver}/T_1) and limit wall temperature difference ($(T_{max} - T_{min})/T_1$) at the mid-span of the blade surface are analyzed. Fig. 6(a) and (b) presents the average wall temperature and limit wall temperature difference at the mid-span of the blade surface under different cooling conditions, respectively. As shown in Fig. 6(a), the average wall temperature is low when the coolant mass flow rate is high or the coolant temperature is low, which implies that higher mass flow rates and lower temperature of the coolant can effectively decrease the blade surface temperature. And the averaged surface temperature decreases linearly with the increases of the coolant mass flow rate. The mechanism of internal convective cooling in the test blade is similar to that of the forced turbulent heat transfer in the pipe. The average *Nu* number representative of the heat transfer characteristic for fully developed turbulent flow in smooth circular tubes can be expressed by Eq. (1):

$$Nu = 0.23\,Re^{0.8}Pr^{0.4} \tag{1}$$

The *Nu* is related with *Re* powered to about 0.8, indicating that the heat transfer will be enhanced with the increase of *Re*. It also can be seen from Fig. 6(a) that only when the temperature of cooling air is as low as about 0.60, the averaged wall temperature could be lower than that cooled by steam. This means that to achieve the same cooling performance, the mass flow rates of the cooling air has to be higher than steam and the temperature of cooling air is lower than the cooling steam. Fig. 6(b) shows the limit wall temperature difference, in which we can see that the higher the values, the worse the uniformity of the thermal load distribution and the higher the thermal-stress of the blade as well. It can be inferred from Fig. 6(b) that cooling steam can cause higher limit wall temperature difference and lead to higher thermal-stress than cooling air under the same operating condition, consequently. Higher temperature of

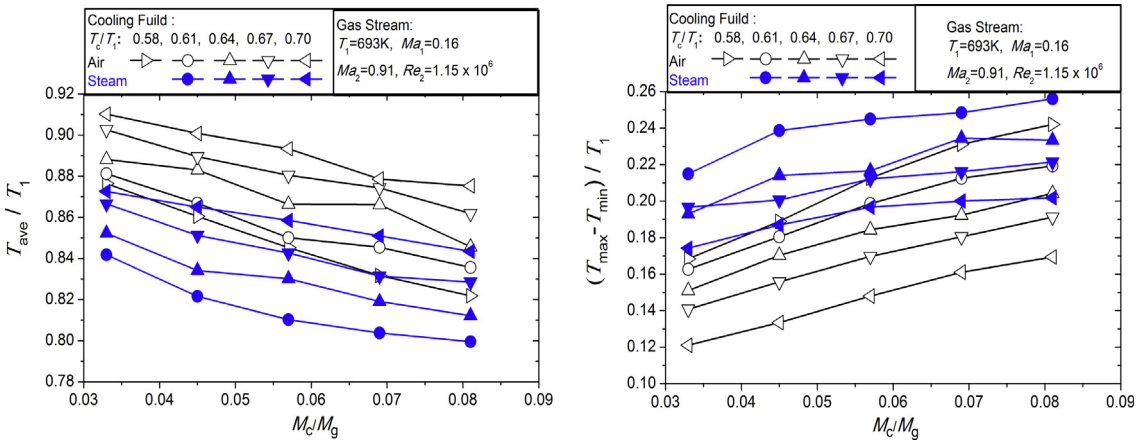

(a) Average wall temperature (b) Limit wall temperature difference

Fig. 6. Average wall temperature and limit wall temperature difference at the mid-span of the test blade.

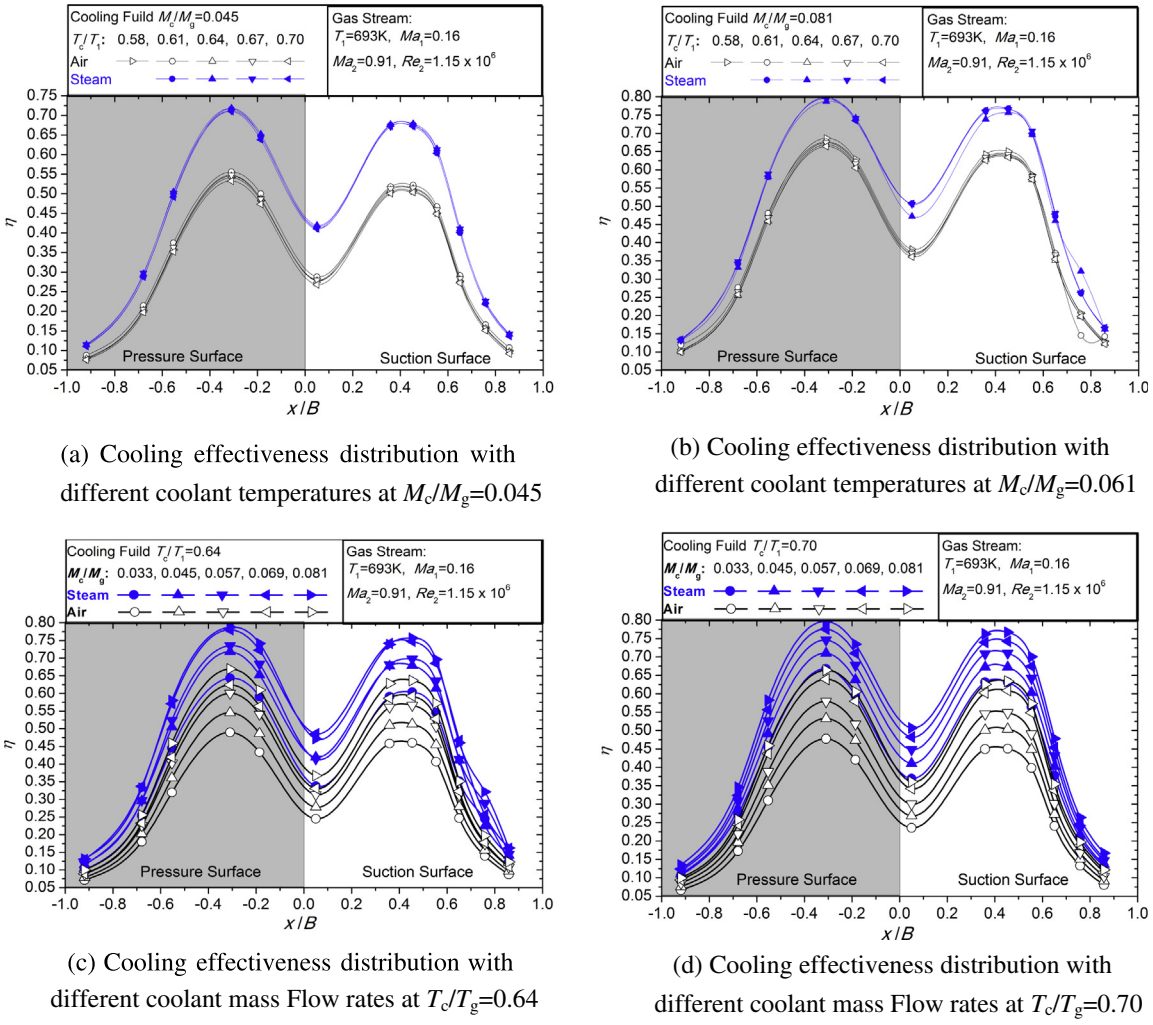

(a) Cooling effectiveness distribution with different coolant temperatures at M_c/M_g=0.045

(b) Cooling effectiveness distribution with different coolant temperatures at M_c/M_g=0.061

(c) Cooling effectiveness distribution with different coolant mass Flow rates at T_c/T_g=0.64

(d) Cooling effectiveness distribution with different coolant mass Flow rates at T_c/T_g=0.70

Fig. 7. Distribution of cooling efficiency at the mid-span of the blade.

coolant can mitigate the limit wall temperature difference. As shown in Fig. 6(b), when the coolant temperature remains unchanged and the mass flow rates rises to a certain range, the value of limit wall temperature difference remains constant.

4.3. Cooling efficiency of the blade

Fig. 7 shows the distribution of cooling efficiency at the mid-span of the test blade. The abscissa is the relative axial chord

length and the ordinate is the cooling efficiency, whose equation is written as below:

$$\eta = (T_1 - T_w)/(T_1 - T_c) \quad (2)$$

Subscript w represents the blade surface. The equation shows that the higher the value, the greater the decrease of the cooled blade surface temperature. When the relative axial chord length is 0.45, the cooling efficiency reaches a maximum of 0.8. The cooling efficiency at the leading area is less than 0.5, and is less than 0.1 at the blade trailing edge. Since the cooling efficiency of the pressure surface is higher than that of the suction surface at the same axial distance, the surface cooling efficiency distribution curves look like an oblique "M" and are symmetric along the leading edge. Fig. 7(a) and (b) shows the cooling effectiveness distribution with different coolant temperatures at $M_c/M_g = 0.045$ and $M_c/M_g = 0.061$, respectively. With the same coolant, the cooling efficiency distribution curves at different coolant temperatures overlap with each other, which indicates that the coolant temperature have no significant impact on the cooling efficiency. This is because Eq. (1) shows that the heat transfer coefficient depends on the Reynolds number and Prandtl number. Though the *Pr* number changes with the coolant temperatures, the coolant temperature has little effect on the cooling performance. Since the temperature range of the coolant is from 129 °C to 212 °C, the Prandtl number of air is ranging from 0.7121 to 0.7118 and from 1.008 to 0.9608 for the steam ranging. Fig. 7(c) and (d) shows the cooling effectiveness distribution with different coolant mass Flow rates at $T_c/T_g = 0.64$ and $T_c/T_g = 0.70$, respectively. The blade cooling effectiveness increases with the increase of the coolant mass flow rates. At $X/B = 0.45$ where the cooling effectiveness is highest, the cooling effectiveness of steam is higher than that of air by about 0.15. As $T_c/T_g = 0.64$, the cooling effectiveness for the air cooling when $M_c/M_g = 0.081$ is slightly higher than that steam cooling when $M_c/M_g = 0.033$. While as $T_c/T_g = 0.70$, the cooling effectiveness for the air cooling when $M_c/M_g = 0.081$ is basically the same as that steam cooling when $M_c/M_g = 0.033$. This may indicate that by using steam cooling, the mass flow rate of coolant can be particularly reduced.

The concept of averaged cooling effectiveness is introduced in particular to evaluate the comprehensive cooling performance of the blade. The averaged cooling efficiency of the blade can be calculated by Eq. (2), but the blade surface temperature T_w in the equation adopts the averaged surface temperature at the mid-span of the test blade. Fig. 8 presents the averaged cooling effectiveness at different cooling operating conditions. It can be seen that, the coolant inlet temperatures has little effect on the averaged cooling effectiveness at the same coolant mass flow rates are the same.

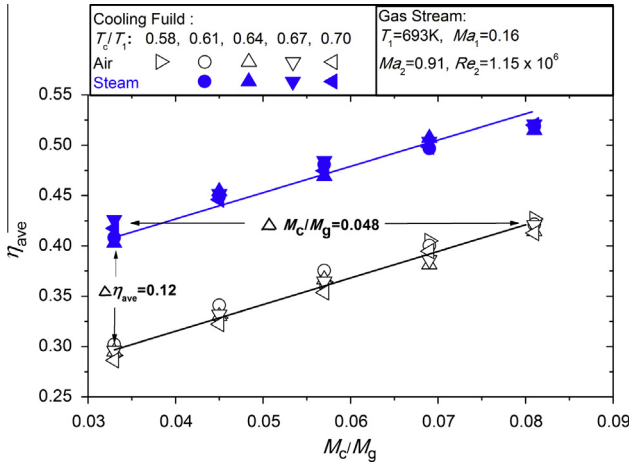

Fig. 8. Averaged cooling effectiveness of the blade middle section.

And the averaged cooling efficiency increases with the coolant mass flow ratio. At the same mass flow rate, the averaged cooling effectiveness of steam cooling is higher than that of air cooling by 0.12. To achieve the same cooling performance, the mass flow ratio of steam coolant is lower than that of air coolant by 0.048.

From the results and analysis above, we can see that steam cooling has higher cooling effectiveness than the air cooling, while the cooling effectiveness at the leading edge and the trailing edge of the blade is still low by using the steam internal convective cooling. Actually in real gas turbine blade cooling the most effective cooling structure for the leading and trailing edge is film cooling, which has to select air as the coolant. So the combination of air cooling and steam cooling will be a better idea. In addition, the steam closed-loop cooling is suitable for the gas–steam combined cycle device, since the steam is easy to get. And the sealing for the steam and steam corrosion will be important problems to solve.

5. Conclusions

The five-smooth-channel internal cooling structure adopted in this study makes the cooling effectiveness reaches the peak value at $X/B = \pm 0.45$. The cooling effectiveness at the trailing edge is the lowest due to the special geometry of the trailing edge and the limitations of the structural strength. So the cooling structure in this study calls for some further improvement. In addition, the cooling effectiveness on the pressure surface is slightly higher than that of the suction surface at the same axial distance. The temperature distribution curves are shaped like an oblique "W" and the cooling efficiency distribution curves are shaped like an oblique "M". Both curves are symmetric along the leading edge.

Blade surface temperature declines with the increase coolant mass flow rate and decreases of coolant temperature. The cooling effectiveness of steam is much higher than the air. At the same mass flow rate, the averaged cooling effectiveness of steam cooling is higher than that of air cooling by 0.12; and to obtain a similar integrated cooling performance, steam coolant has to consume only 40.82% of the mass flow rate that air coolant has to consume. In conclusion, steam coolant has a better cooling effect than air under the same condition. However, steam cooling may cause larger thermal-stresses. To relieve the thermal-stress, lower cooling mass flow rates and higher coolant temperature have to be used for the same coolant.

Acknowledgments

The research work was supported by National Natural Science Foundation of China (51106124) and Doctoral Program of Higher Education Research Fund (20100201120007).

References

[1] Han, Je-Chin, Chen, Hamn-Ching, Turbine Blade Internal Cooling Passages with Rib Tabulators, American Institute of Aeronautics and Astronautics, Reston, VA, ETATS-UNIS, 2006.
[2] S. Gupta, A. Chaube, P. Verma, Review on heat transfer augmentation techniques: application in gas turbine blade internal cooling, J. Eng. Sci. Technol. Rev. 5 (2012) 57–62.
[3] P. de la Calzada, J.J. Alvarez, Experimental investigation on the heat transfer of a leading edge impingement cooling system for low pressure turbine vanes, J. Heat Transfer 132 (2010).
[4] A.C. Chambers, D.R. Gillespie, P.T. Ireland, M. Mitchell, Enhancement of impingement cooling in a high cross flow channel using shaped impingement cooling holes, ASME (2006).
[5] T. Horbach, A. Schulz, H.-J. Bauer, Trailing edge film cooling of gas turbine airfoils – external cooling performance of various internal pin fin configurations, J. Turbomach. 133 (2011).
[6] S. Yamawaki, C. Nakamata, R. Imai, S. Matsuno, T. Yoshida, F. Mimura, M. Kumada, Cooling performance of an integrated impingement and pin fin cooling configuration, ASME (2003).

[7] M. Arai, T. Suidzu, Porous ceramic coating for transpiration cooling of gas turbine blade, J. Therm. Spray Technol. (2013) 1–9.
[8] Z. Gao, D. Narzary, S. Mhetras, J.-C. Han, Full-coverage film cooling for a turbine blade with axial-shaped holes, J. Thermophys. Heat Transfer 22 (2008) 50–61.
[9] S.H. Oh, D.H. Lee, K.M. Kim, M.Y. Kim, H.H. Cho, Enhanced cooling effectiveness in full-coverage film cooling system with impingement jets, ASME (2008).
[10] L.D. Hylton, M.S. Mihelc, E.R. Turner, D.A. Nealy, R.E. York, Analytical and experimental evaluation of the heat transfer distribution over the surfaces of turbines blades, NASA CR (1983) 168015.
[11] E.P. John, H system TM technology update, ASME (2003) 903–912.
[12] E. Bancalari, I.S. Diakunchak, G. McQuiggan, A Review of W501G engine design, development and field operating experience, ASME (2003) 925–932.
[13] Y. Fukuizumi, J. Masada, V. Kallianpur, Y. Iwasaki, Application of H gas turbine design technology to increase thermal efficiency and output capability of the Mitsubishi M701G2 gas turbine, J. Eng. Gas Turbines Power 127 (2005) 369–374.
[14] I. Sato, 1500 °C Class "H" gas turbine combined-cycles, J. Jpn. Inst. Energy 86 (7) (2007) 443–446.
[15] C. Koeneke, Steam cooling nears a commercial milestone, Power 149 (2005) 31–35.
[16] B. Macdonnell, P. McDonough, K. Boral, Y. Fukuizumi, Steam cooling hits the mark, Power Eng. Inter. 14 (2006).
[17] K. Jordal, J. Fridh, L. Hunyadi, M. Jönsson, U. Linder, New possibilities for combined cycles through advanced steam technology, ASME (2002).
[18] O. Singh, B. Prasad, Comparative evaluation of gas turbine power plant performance for different blade cooling means, Proc. Inst. Mech. Eng., Part A: J. Power Energy 223 (2009) 71–82.
[19] M.H. Albeirutty, A.S. Alghamdi, Y.S. Najjar, Heat transfer analysis for a multistage gas turbine using different blade-cooling schemes, Appl. Therm. Eng. 24 (2004) 563–577.
[20] S. Ausmeier, W. Bitterlich, P. Winske, Effect of evaporation cooling of gas turbine blades on design, efficiency and economy, Euro. J. Mech. Environ. Eng. 46 (2001) 229–236.
[21] H. Nomoto, A. Koga, S. Ito, Y. Fukuyama, F. Otomo, S. Shibuya, M. Sato, Y. Kobayashi, H. Matsuzaki, The advanced cooling technology for the 1500 C class gas turbines: steam-cooled vanes and air-cooled blades, J. Eng. Gas Turbines Power 119 (1997) 624–632.
[22] P.D. Henderson, An experimental research on analysis of using steam for cooling turbine blades. Ann Arbor: Michigan State University, 1997.
[23] Ramakrishnan Pudupatty. Comparison of the cooling effectiveness of superheated steam and hot air in internal turbine blade cooling. Ann Arbor: Michigan State University, 1998.
[24] D. Bohn, A. Wolff, M. Wolff, K. Kusterer, Experimental and numerical investigation of a steam-cooled vane, ASME (2002).
[25] D. Bohn, J. Ren, K. Kusterer, Investigation of the steam-cooled blade in a steam turbine cascade, J. Aerospace Power 22 (2007).
[26] G. Nowak, W. Wroblaewski, I. Nowak, Convective cooling optimization of a blade for a supercritical steam turbine, Int. J. Heat Mass Transf. 55 (2012) 4511–4520.
[27] W. Wang, J. Gao, X. Shi, L. Xu, Cooling performance analysis of steam cooled gas turbine nozzle guide vane, Int. J. Heat Mass Transf. 62 (2013) 668–679.
[28] W. Wang, J.M. Gao, X.J. Shi, et al., Experimental study on comparison of cooling effectiveness between steam and air for a gas turbine nozzle guide vane, ASME (2012) 255–263.
[29] S.J. Kline, F.A. McClintock, Describing uncertainty in single sample experiments, Mech. Eng. 75 (1953) 3–8.